Hindawi
International Journal of Antennas and Propagation
Volume 2019, Article ID 8090936, 10 pages
https://doi.org/10.1155/2019/8090936

Research Article

Design of a Compact Ultrawideband U-Shaped Slot Etched on a Circular Patch Antenna with Notch Band Characteristics for Ultrawideband Applications

Jiwan Ghimire and Dong-You Choi

Department of Information and Communication Engineering, Chosun University, 375 Susuk-dong, Dong-gu, Gwangju 501-759, Republic of Korea

Correspondence should be addressed to Dong-You Choi; dychoi@chosun.ac.kr

Received 29 September 2018; Accepted 26 December 2018; Published 18 February 2019

Academic Editor: Claudio Gennarelli

Interference between ultrawideband (UWB) antennas and other narrowband communication systems has spurred growth in designing UWB antennas with notch characteristics and complicated designs consisting of irregular etched slots and larger physical size. This article presents a simplified notched design method for existing UWB antennas exhibiting four frequency-band-rejecting characteristics. The investigation has been conducted by introducing four semicircular U-shaped slot structures based on a theoretical formulation. The formulation is validated with the equivalent LC lumped parameters responsible for yielding the notched frequency. A novel feature of our approach is that the frequency notch can be adjusted to the desired values by changing the radial length based on the value calculated using a derived formula for each semietched U-slot, which is very simple in structure and design. Additionally, by introducing the rectangular notch at the ground plane, the upper passband spectrum is suppressed while maintaining the wide impedance bandwidth of the antenna applicable for next-generation wireless communications, 5G. The measured result shows that the antenna has a wide impedance bandwidth of 149% from 2.9 to 20 GHz, apart from the four-notched frequencies at 3.49, 3.92, 4.57, and 5.23 GHz for a voltage standing wave ratio (VSWR) of <2 rejecting the Worldwide Interoperability for microwave Access (WiMAX) band at (3.38-3.7 GHz), the European C-band at (3.84-4.29 GHz), the Indian national satellite (INSAT) at (4.47-4.92 GHz), and wireless local area networks (WLANs) at (5.09-5.99 GHz). Measured and simulated experimental results reveal that the antenna exhibits nearly an omnidirectional pattern in the passband, low gain at the stopband, and good radiation efficiency within a frequency range. The LC equivalent notched frequency has been proposed by analyzing the L and C equivalent formula, and it has been validated with simulated and measured results. The measurement and simulated results correspond well at the LC equivalent notch band rejecting the existing narrowband systems.

1. Introduction

Modern wireless communication systems use the ultrawideband (UWB) system because of its advantages of smaller size, lesser complexity, and its provisioning for various service applications on different frequency bands with high-speed data rates and high time-domain resolution. Furthermore, multiband UWB microstrip patch antennas are popular for their simple features, including low profile, low manufacturing cost, simple feeding, and easy integration with active circuit components [1–3]. Moreover, the demand of various service applications within the same antenna, such as a multinotch frequency band for mitigating interference with other narrowband communication systems, has inspired the development of miniaturized antennas that are compact and simple in design complexity. Because the antenna requires less power, it can be integrated with other portable Internet of Things (IoT) applications, surveillance systems, wireless body area networks (WBANs), and sensing and imagining applications that support all the data communication system bands [4–7]. However, because of the many wide bands working under the UWB system, collision of these narrow

bands (e.g., the Worldwide Interoperability for microwave Access (WiMAX) operating at 3.3–3.6 GHz, the European C-band at 3.8–4.2 GHz, the Indian national satellite (INSAT) at 4.50–4.80 GHz, and wireless local area networks (WLANs) at 5.15-5.825 GHz) is inevitable. Solving this problem may give rise to complications of increased size and cost and insertion loss for the UWB system. As a remedy for this situation, in this paper, we present a new design approach of adding U-shaped etched slot structure based on formulated slot characteristics and LC equivalent notched frequency results for multiband rejection to the UWB antenna.

Band notch antenna techniques by etching thin slots in the radiating surface of an antenna or ground plane can be used for making multiband antennas and producing a notch at lower frequencies by prohibiting interference between UWB and other narrowband systems without any increase in size or additional expenses. To suppress such potential interference, several design configurations have been proposed by modifying either the ground or the radiating patch or both by grooving various shapes (e.g., etching L-shaped, F-shaped, E-shaped, U-shaped, arc-shaped, or circular-shaped slots) to achieve the desired characteristics [8–16]. Adopting electrical and mechanical methods, as well as active filtering elements such as p-i-n diodes and varactor diodes, in different design methods enables reconfigurable antennas to be fabricated in terms of frequency band polarization and pattern and multipattern responses. However, the increased complexity, losses, and size of the system, coupled with the high power requirement, finally degrade the antenna electromagnetic (EM) characteristics [17]. Therefore, designing a UWB antenna using etching techniques for band-rejecting capabilities is the most suitable and economical solution to the problem. Triple-notch frequencies [18, 19], dual-notch frequencies [20–22], and single-notch frequencies [23–25] have been proposed using various design configurations either by adding tuning stubs or by etching slots. The addition of etching slots changes the current distribution and characteristic impedance along the radiating surface, contributing to perturbations in radiating modes by subsequently reducing the size of the antenna for realizing the given resonant frequency with a decreased quality factor (Q) value and proportionally increasing the bandwidth or establishing dual-band functionality [26]. However, placing the slots irregularly with a complex configuration in a radiating patch or a ground plane complicates the job of localizing the slots in the design and adds iteration time to the simulation design, making the process tedious. In addition, developing efficient bandwidth enhancement with the band-notching technique in an area of limited size is still a difficult task.

This paper describes a simple method to design a frequency-notched UWB antenna by adding a semicircular slot etched on the radiating patch surface. The notched frequency is tuned by changing the radius of the semicircular slot and the vertical etched slot whose length is half of the corresponding semicircular etched slot's radius. This arrangement is used to filter the unwanted frequency and avoid potential interference from narrowband communication systems within the UWB. In this paper, we present the UWB effect by introducing slots on the antenna and compare the formulated notched frequency with the equivalent LC lumped model notch frequency. The study of the antenna is conducted via a simulation with Ansoft High-Frequency Structure Simulator (HFSS), a commercial electromagnetic simulator, and the optimized parameters are specified in Table 1. The antenna with a size of 25 mm × 25 mm × 1.62 mm is designed on a Taconic substrate and connected to a 50 Ω feedline. The feedline and patch are separated from the ground plane by the same length.

Table 1: Optimal dimensions of the proposed antenna.

Parameter	Value (mm)	Parameter	Value (mm)
L_S	25	R_1	4.12
W_S	25	R_2	4.705
H_S	1.62	R_3	5.484
G_L	5	R_4	6.2
F_L	5.38	L_1	2.06
F_W	2.5	L_2	2.35
R_p	10.3	L_3	2.74
G_1, G_2, G_3, G_4, G	0.38	L_4	3.1
S_L	1.2	S_W	2.8

2. Antenna Design

Figure 1 shows the dimensions and geometry of the designed antenna. The antenna consists of a monopole circular patch with radius $R_p = 10.3$ mm and feedline length $F_L = 5.38$ mm printed on a Taconic substrate with relative permittivity (ε_r) of 4.5 and a loss tangent of 0.0035. The ground plane serves as the impedance-matching circuit, whose impedance depends upon its width as current is mainly distributed at its upper edge [27]. The length of the ground plane (G_L) is adjusted to nearly half of the radius of the radiating circular patch, whereas the antenna width is varied till the characteristic impedance bandwidth of VSWR < 2 at lower frequency bands is obtained. A small rectangular notch is etched on the ground plane below the feedline to create a capacitive load that nullifies the inductive nature of the patch antenna and produces nearly resistive input impedance, especially at a higher band. Here, the return loss at the 10 dB lower frequency bandwidth is closely adjusted to $\lambda/4$ of the total combined length of the circular patch and feedline. Four semicircular slots, of optimized radii of $R_1 = 4.12$ mm, $R_2 = 4.705$ mm, $R_3 = 5.484$ mm, and $R_4 = 6.2$ mm, are etched along with the vertical slot, each having a length half of the consecutive semicircular slot radius. The center of each semicircular slot is the same to that of the radiating circular patch. The formulated notch frequency for the related dimension is calculated in the following section as [28]

$$f_n = \frac{C}{2S_n\sqrt{(\varepsilon_r + 1)/2}}, \quad (1)$$

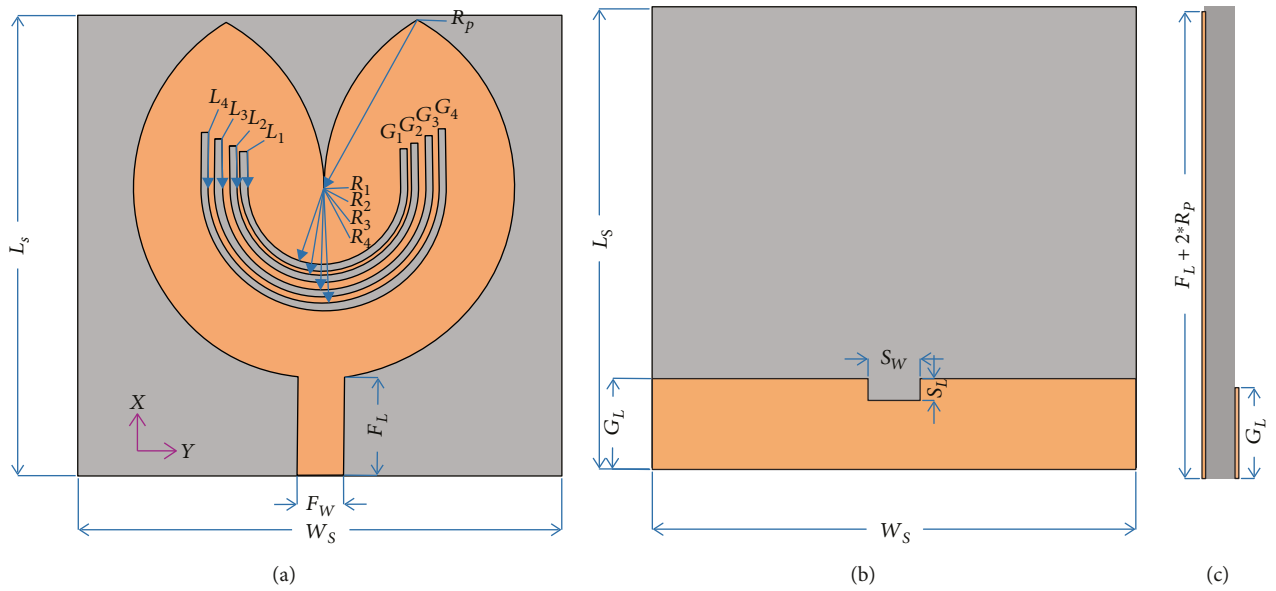

FIGURE 1: Proposed design. (a) Top view. (b) Back view. (c) Side view.

where f_n is the notch frequency, c is the speed of light, and ε_r is the relative permittivity of the substrate. The effective lengths S_n for notches n from 1 to 4 are made nearly equal to half of the guided wavelength at the notched frequency of the band and are calculated as

$$S_n = \pi\left(R_n + \frac{G}{2}\right) + 2L_n - G, \tag{2}$$

where L_n is the slot's vertical length, which is half of the value of the radius R_n, and G is the width of the etched slot. Because of the fringing fields in the etched slot, the effective electrical length of the radiating patch within an etched plane gets increase than its physical length and hence the effective width of the slot gap gets decrease, so the total effective radius is approximated to be the sum of the physical length of the radius R_n and the mean of slot width G. Similarly, because of fringing at the end of the vertical stub, its physical length gets reduced by the mean slot width. Overall, the effective lengths of each etched slot will be the sum of electrical length of semicircular slots and two vertical stubs of length reduced by slot width.

The optimized notching radii are selected based on a graph plotted between frequency and radii using equations (1) and (2) as formulated notched frequency and equations (3)–(7) as LC equivalent notch frequency. Figure 2 gives the graphical relation between the formulated notch frequency and the LC equivalent notch frequency and shows that the formulated and LC equivalent notch frequencies are almost close to each other for every semicircular etched radius. The radius from the graph as determined with respect to each desired notch frequency is then used in the simulation and antenna fabrication and the results from the simulated notched frequency are compared to the measured results in Table 2.

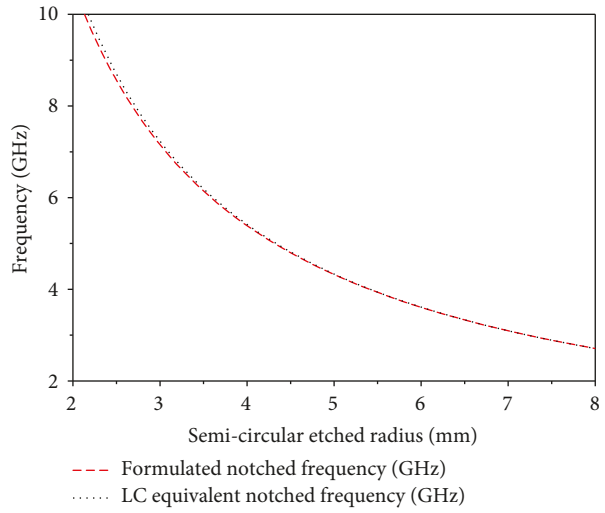

FIGURE 2: Graph of a formulated (f_n) vs. LC equivalent (f_0) notched frequency with respect to semicircular etched radius based on equations (1) and (3).

The LC equivalent notch resonant frequency f_0 of the etched slot is given by

$$f_0 = \frac{1}{2\pi}\sqrt{\frac{1}{L_{\text{eq}}C_{\text{eq}}}}, \tag{3}$$

where C_{eq} is the total equivalent capacitance of the slot structure, which is the sum of the combination of capacitances of the semicircular slot and the two vertical etched

Table 2: Comparison of LC equivalent lumped element with simulated, measured, and formulated notch frequency.

Notches	R_n (mm)	Simulated notched frequency (GHz)	Measured notched frequency (GHz)	Formulated theoretical frequency (GHz)	Parameter L (nH)	Parameter C (pF)	LC equivalent notch frequency (GHz)
1	4.12	5.32	5.23	5.23	67.278	0.0139	5.25
2	4.705	4.68	4.57	4.58	76.553	0.0158	4.6
3	5.484	4.03	3.93	3.94	88.904	0.0185	3.94
4	6.2	3.57	3.49	3.49	100.257	0.02	3.49

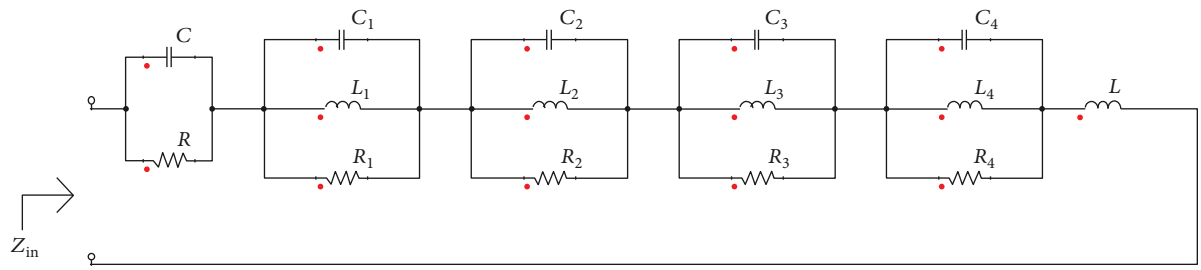

Figure 3: Equivalent lumped element circuit model of a slot etched antenna.

slots, along with the surface capacitance resulting from the charge on the surface of the etched slot. C_{eq} can be evaluated from [29]

$$C_{eq} = \varepsilon_0 \left[\frac{\pi R_n t_P}{G} + \frac{2\pi t_P}{\ln\left((2\times 4t_P)/\pi R_n\right)}\right] + 2\varepsilon_0 \left[\frac{L_n t_P}{G} + \frac{2\pi t_P}{\ln\left((2\times 4t_P)/2L_n\right)}\right] + \frac{2\varepsilon_0 t_p}{\pi}\left[\ln\left(\frac{4P}{G}\right)\right], \quad (4)$$

where t_P is the thickness of the patch (generally 35 μm for a Taconic substrate) and G is the etched slot in the metallic patch, which is set the same for every etched slot. The slot length L_n is the vertical length, which is half the semicircular radius as mentioned earlier. The first section of the right side of equation (4) is the parallel-plate capacitance resulting from air in the gap, the second part is a correction owing to fringing of the electric field at the etched slot edges, and the last section is the total surface capacitance resulting from the patch thickness and is calculated by assuming $P = G/2$. The equivalent inductance (L_{eq}) for the notched surface can be calculated by assuming the notch area as a wire of rectangular cross section having finite length E and thickness D in length equal to half of the slot's radius as proposed in [30] as

$$L_{eq} = 0.0002E\left(2.303\log_{10}\left(\frac{4E}{D}\right) - \theta\right)\mu H, \quad (5)$$

where the constant $\theta = 2.451$ is for a slot structure of circular geometry and depends upon the shape of the loop structure. Because the maximum etched portion has a semicircular geometry, the constant for the vertical slot that has a wire loop of square is assumed to be equal to that of a semicircle and is included inside of the semicircular

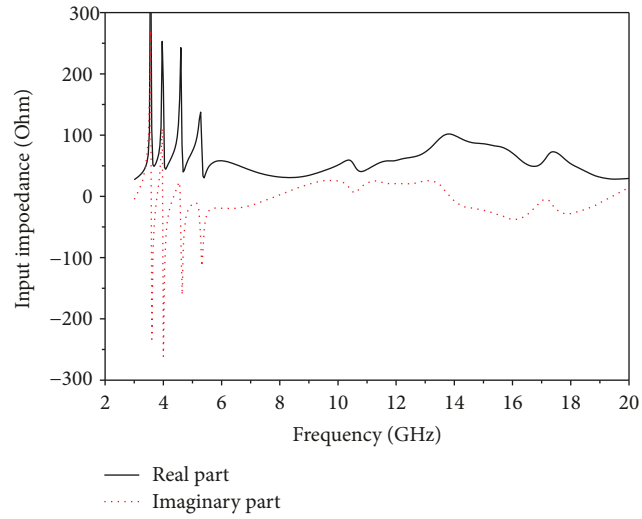

Figure 4: Input impedance of the proposed antenna.

geometry for calculation. The length E and D can be evaluated as

$$E = 2S_n + G, \quad (6)$$

$$D = \frac{R_n}{2}. \quad (7)$$

The effective lengths S_n for notches n is derived from equation (2). Both the above equations are based on the analysis of the resonant frequency of a split ring and a simplified loop formula for regular figures. The parameters of the equations are based on the configuration of an etched slot structure. Because of the perturbation of

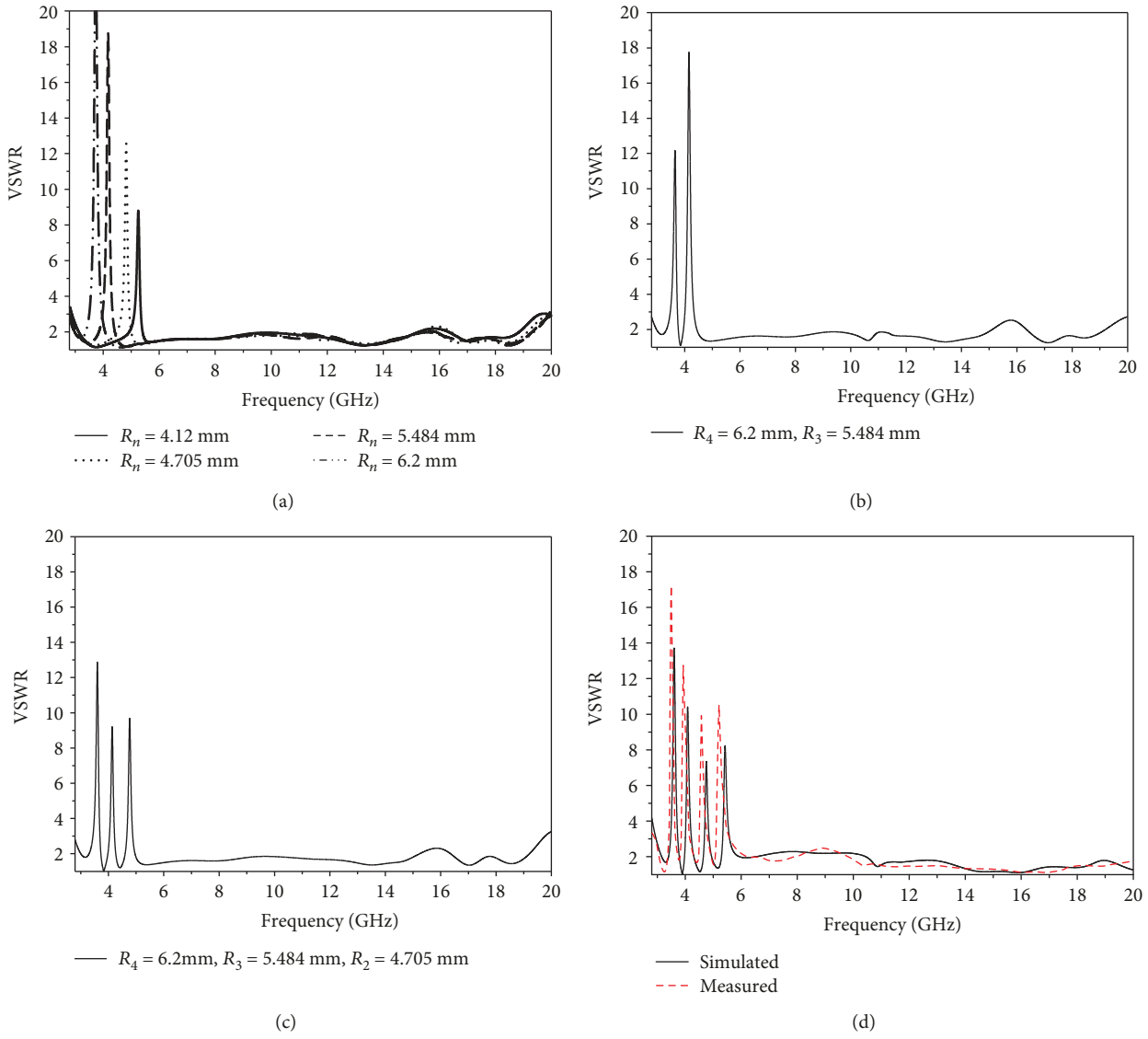

Figure 5: Notch frequency for different geometrical etched slot parameters. (a) Notch at the different frequency band from varying the parameter R_n. (b) Notch at the WiMAX band and the C-band from parameters R_4 and R_3. (c) Notch at the WiMAX band, the European C-band, and INSAT band from parameters R_4, R_3, and R_2. (d) Measured and simulated frequency notch at the WiMAX band, the European C-band, INSAT band, and WLAN band from parameters R_4, R_3, R_2, and R_1.

the current distribution on the radiating patch by etching, the current has to take a longer path. This path determines the series inductance, whereas the thin gap of the etch is responsible for the accumulation of charge and consequently formation of the series capacitance [31]. This combined effect can be shown by the equivalent LC parameter lumped element circuit, which is expressed in equations (4) and (5). The equivalent lumped element parallel RLC circuit model of the proposed antenna is shown in Figure 3. L_i, C_i, and R_i for ($i = 1$ to 4) are the inductance, capacitance, and radiation resistance for ith radiating mode at each resonant frequency band, respectively. Each etched slot has a lumped effect that attenuates the frequency band and can be represented as a series combination of every four lumped elements with a notched ground plane as a capacitive load and an inductive radiating patch. Capacitive (C) and inductive (L) effects are taken into account for higher order modes as well as feeding effect and are the dominant term for the input impedance of the antenna. In Figure 4, we see the equivalent input impedance (Z_{in}) of the antenna; the resistance varies around 50 Ω while its input reactance oscillates around zero. The maximum equivalent resistance is found in the notch bands while the equivalent reactance almost tends to zero. This is due to the RLC resonating condition, where capacitive impedance is equal to inductive impedance, which gets cancelled out, as the resistance part takes on that role. Impedance mismatch between the feedline and the radiating patch is responsible for the band-rejecting characteristics.

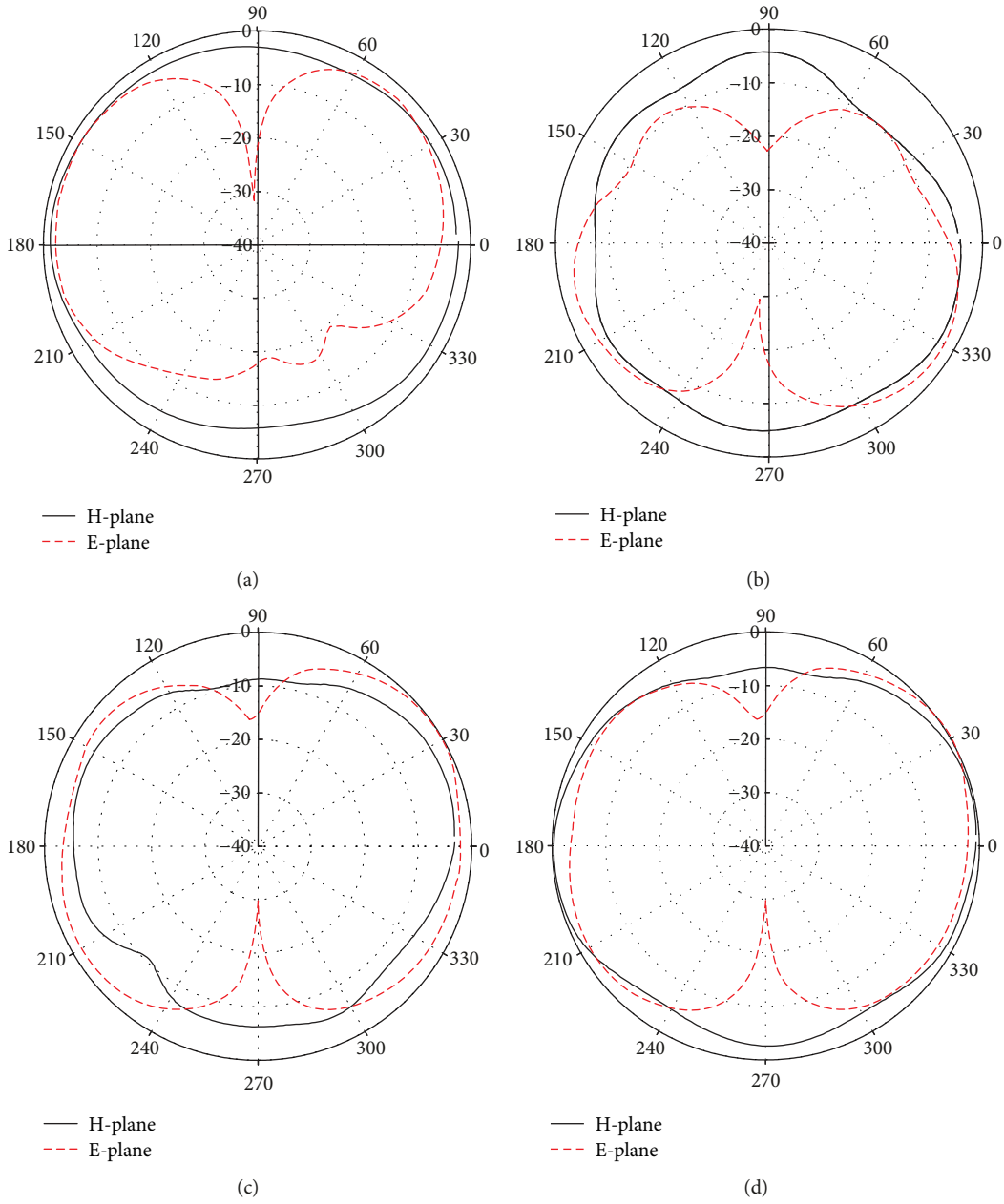

Figure 6: Measured radiation pattern of the proposed antenna. (a) 3.26 GHz. (b) 3.77 GHz. (c) 4.41 GHz. (d) 5.02 GHz.

3. Design Strategy

By using the layout of the prototype antenna shown in Figure 1, the individual effect of each etched slot of radial length R_n in a radiating patch on the voltage standing wave ratio (VSWR) is shown in Figure 5(a). The experiments are made on a Taconic substrate of relative permittivity $(\varepsilon_r) = 4.5$ with etched slots of 0.38 mm in width. By tuning the parameters R_1, R_2, R_3, and R_4, one can get the first, second, third, and fourth resonating frequencies for WiMAX, the European C-band, INSAT, and WLANs easily. Because the resonating frequency completely depends on the semicircular etched slot's radial length, we can shift the notching frequency to any desired ones. The plots from the graph as shown in Figure 2 give the slot radial length and this is taken into account in the simulation for the required corresponding notch frequency. Figure 5 shows the VSWR plots of various etched slots of differing radial parameter. The increase in the VSWR at the notched frequency stopband can ensure high-quality UWB communication links by filtering coexisting narrowband interference. The frequency notches for consecutive slots are relatively less affected by the neighboring slots in terms of coupling issues, as each resonator slot is physically far away from another, being at least beyond the fringing field of each slot. Results from Table 2 comparing the LC equivalent notch frequency with respect to the simulated notched frequency also demonstrate that successive slots are relatively less affected by neighboring slots.

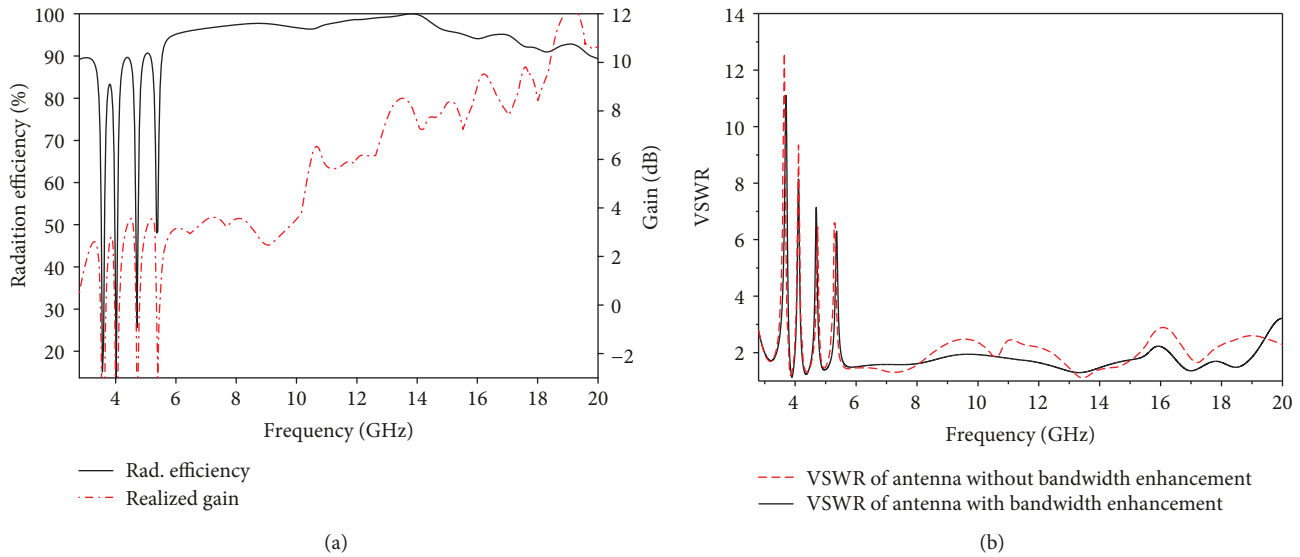

FIGURE 7: (a) Simulated antenna gain and radiation efficiency and (b) simulated VSWR plot of the UWB antenna with ground notch versus without notch for bandwidth enhancement.

Table 2 compares the formulated, simulated, and measured notched frequency with the equivalent model of an LC lumped element circuit, represented by four parallel RLC resonators connected in series. At resonating conditions, the stopband frequency or cutoff frequency depends upon L and C, and it can be evaluated using equations (4) and (5). The lumped element equivalent resonance notched frequency computed using equation (3) corresponds well with the measured and formulated values.

4. Results

4.1. Antenna Gain and Radiation Efficiency. The proposed antenna's final measured radiation patterns are shown in Figure 6. The measurements were taken in an anechoic chamber covering different passbands of the UWB. The radiation pattern in the x-z plane (E plane) is bidirectional and it is nearly omnidirectional in the y-z plane (H plane), which shows that the antenna radiates over a range of frequencies with minimum effect of band notching behavior on the antenna radiation patterns.

From Figure 7(a), we can see that different etched slots on the antenna yield well-suppressed antenna gain and efficiency at the four places of the intended rejection band, indicating high interference at those frequencies. This clearly specifies the band-rejection characteristics of the semicircular etched slot. Figure 7(b) depicts the change in impedance bandwidth by adding rectangular notch of length S_L and width S_w at the ground plane. By etching a small rectangular surface at the ground, beneath the feedline of the radiating patch, radical improvement in the bandwidth performance of the antenna was obtained which is suitable for working at emerging next-generation wireless communication, 5G. And also, when adding notch at the ground plain, it is seen that the effects on the notched frequency bands are negligible. Figure 8 shows the simulated surface current distribution at each rejection band; it can be seen that the surface current is concentrated mainly on the periphery of each semietched slot, which acts as a resonator, prohibiting signal propagation at that frequency.

4.2. Comparison of Proposed Antenna with Other References. To validate the performance of the antenna, a comparison is made in Table 3 with other reported antennas owing the advantage of smaller size, a wider impedance bandwidth, and complete rejecting bands with maximum VSWR parameter. As most of the antenna reported in the literature have irregularly placed parasitic stubs and resonators with asymmetrical etching on the radiating and ground surfaces as well as complexity in manufacturing design and structure, our proposed antenna has much advantage of placing regular symmetrical etched slot which is easy to tune, replicate, and fabricate for the desired notch frequency bands.

5. Conclusion

In this paper, a microstrip-fed UWB antenna with four-band notch characteristics is proposed. First, a UWB antenna was designed to have a 149% bandwidth and operate from 2.9 to 20 GHz by inserting small notches in the ground plane to suppress the upper passband spectrum. Second, four U-shaped slots on the radiating patch were introduced to yield four-band notching to mitigate the electromagnetic interference with WiMAX, the European C-band, INSAT, and WLANs by using the design guidelines that are discussed with corresponding equations. LC equivalent equations are proposed based on analyzing split rings and loop formulas for regular figure. This methodology allows the antenna designer to choose the selective frequency for rejection and therefore adapt the radiating patch antenna to reject any narrowband system requirement. The measured results from the proposed antenna correspond well with the simulated,

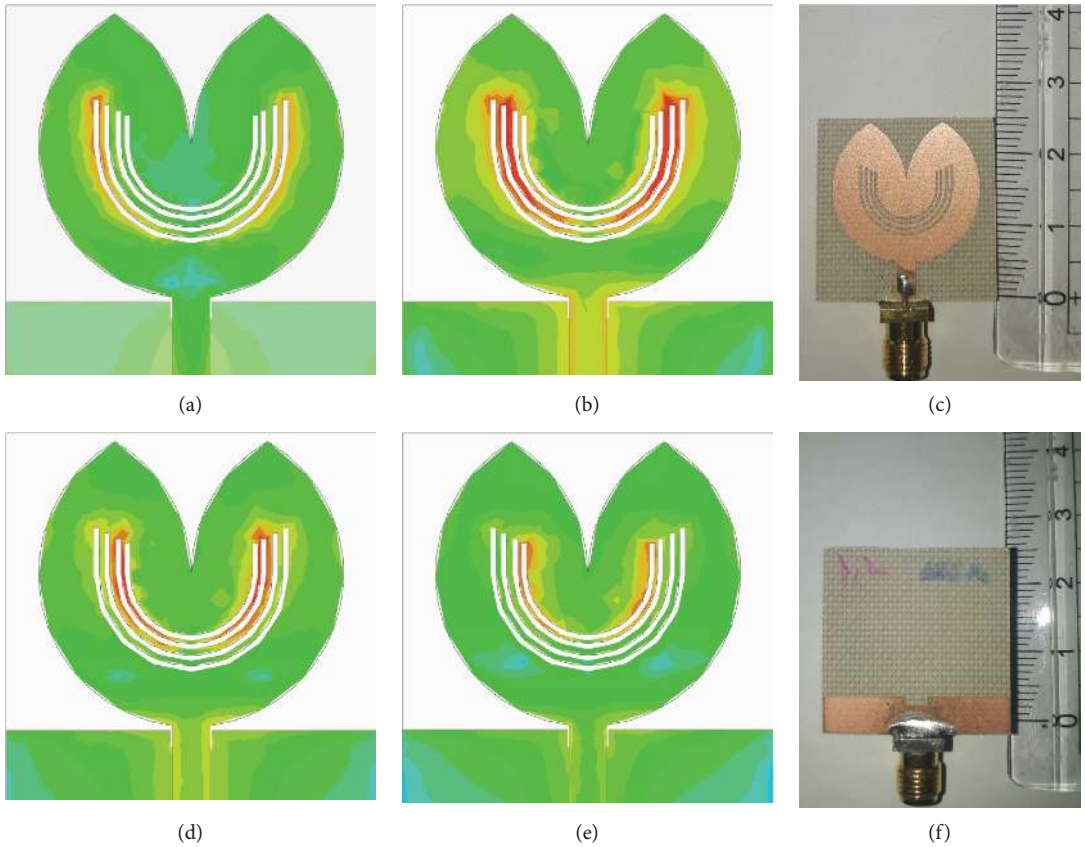

Figure 8: Simulated surface current distribution on the radiating patch of the proposed antenna at the corresponding central frequency of the notched band at (a) 3.57 GHz, (b) 4.03 GHz, (d) 4.68 GHz, and (e) 5.32 GHz. Prototype of the fabricated antenna. (c) Front view. (f) Back view.

Table 3: Comparison of the proposed antenna with other reported references.

References	Size (mm)	Bandwidth (GHz)	Notched bands (GHz)
[20]	20 × 27	2.89-11.52	3.4-3.69, 5.15-5.825
[21]	24 × 28	3.0-13.0	5.15-5.4, 5.725-5.94
[22]	38.5 × 46.4	2.0-12.5	5.0-5.5, 7.2-7.6
[23]	27 × 20	3.1-10.6	5.15-5.85
[24]	22 × 8.5	3.8-10.6	5.15-5.85
[25]	30 × 28	2.78-12.3	5.2-6.0
[32]	31 × 33	2.0-6.0	3.19-3.97, 4.92-5.86
[33]	66.3 × 66.3	3.1-10.6	3.6-3.9, 5.6-5.8
[34]	30.2 × 25	2.7-12.3	3.19-3.97, 5.16-5.85, 7.88-8.59
[35]	30 × 30	3.04-10.9	3.29-3.61, 4.65-5.49, 7.3-8.41
[36]	28 × 26	3.1-12.0	5.15-5.35, 5.75-5.85, 7.25-7.75, 8.01-8.55
[37]	40 × 40	2.1-11.0	2.37-2.9, 3.27-3.76, 5.2-5.89, 8.06-8.8
[38]	30 × 28	3.0-11.0	3.3-3.6, 4.5-4.8, 5.15-5.35, 5.7-5.825
Proposed work	25 × 25	2.9-20.0	3.38-3.7, 3.84-4.29, 4.47-4.92, 5.09-5.99

theoretical, and LC equivalent analytical notch results. The performance of the antenna is good, with decent impedance matching and VSWR < 2, except at the notch bands. Overall, the presented antenna is suitable for working in a UWB communication system and sensing application, rejecting the narrowband notched frequency.

Data Availability

The data used to support the findings of this study are available from the corresponding author upon request.

Conflicts of Interest

The authors declare that they have no competing interests.

References

[1] J. Chóliz, Á. Hernández, and A. Valdovinos, "A framework for UWB-based communication and location tracking systems for wireless sensor networks," *Sensors*, vol. 11, no. 9, pp. 9045–9068, 2011.

[2] J. Zhang, P. V. Orlik, Z. Sahinoglu, A. F. Molisch, and P. Kinney, "UWB systems for wireless sensor networks," *Proceedings of the IEEE*, vol. 97, no. 2, pp. 313–331, 2009.

[3] S. A. Aghdam, "Reconfigurable antenna with a diversity filtering band feature utilizing active devices for communication systems," *IEEE Transactions on Antennas and Propagation*, vol. 61, no. 10, pp. 5223–5228, 2013.

[4] A. Bekasiewicz and S. Koziel, "Compact UWB monopole antenna for internet of things applications," *Electronics Letters*, vol. 52, no. 7, pp. 492–494, 2016.

[5] B. Allen, M. Dohler, E. Okon, W. Malik, A. Brown, and D. Edwards, *Ultra-Wideband Antennas and Propagation: For Communications, Radar and Imaging*, John Wiley & Sons, 2006.

[6] K. Y. Yazdandoost and R. Kohno, "UWB antenna for wireless body area network," in *2006 Asia-Pacific Microwave Conference*, pp. 1647–1652, Yokohama, Japan, December 2006.

[7] G. Adamiuk, T. Zwick, and W. Wiesbeck, "UWB antennas for communication systems," *Proceedings of the IEEE*, vol. 100, no. 7, pp. 2308–2321, 2012.

[8] J. Marimuthu and M. Esa, "Compact UWB PCML bandpass filter with L- and C-shaped resonator," *Electronics Letters*, vol. 44, no. 6, pp. 419-420, 2008.

[9] E. Jung, J. W. Lee, and C. S. Cho, "Signal distortion analysis of L-shaped UWB antenna," *IEEE Antennas and Wireless Propagation Letters*, vol. 9, pp. 775–778, 2010.

[10] A. K. Gautam, L. Kumar, B. K. Kanaujia, and K. Rambabu, "Design of compact F-shaped slot triple-band antenna for WLAN/WiMAX applications," *IEEE Transactions on Antennas and Propagation*, vol. 64, no. 3, pp. 1101–1105, 2016.

[11] J. H. Lu and C. H. Yeh, "Planar broadband arc-shaped monopole antenna for UWB system," *IEEE Transactions on Antennas and Propagation*, vol. 60, no. 7, pp. 3091–3095, 2012.

[12] M. Rahman, "CPW fed miniaturized UWB tri-notch antenna with bandwidth enhancement," *Advances in Electrical Engineering*, vol. 2016, 7 pages, 2016.

[13] A. K. Horestani, Z. Shaterian, J. Naqui, F. Martín, and C. Fumeaux, "Reconfigurable and tunable S-shaped split-ring resonators and application in band-notched UWB antennas," *IEEE Transactions on Antennas and Propagation*, vol. 64, no. 9, pp. 3766–3776, 2016.

[14] J. Liu, K. P. Esselle, and S.-S. Zhong, "A printed extremely wideband antenna for multi-band wireless systems," in *2010 IEEE Antennas and Propagation Society International Symposium*, pp. 1–4, Toronto, ON, Canada, July 2010.

[15] L. Lizzi, F. Viani, R. Azaro, and A. Massa, "Optimization of a spline-shaped UWB antenna by PSO," *IEEE Antennas and Wireless Propagation Letters*, vol. 6, pp. 182–185, 2007.

[16] S. Yadav, A. K. Gautam, and B. K. Kanaujia, "Design of dual band-notched lamp-shaped antenna with UWB characteristics," *International Journal of Microwave and Wireless Technologies*, vol. 9, no. 02, pp. 395–402, 2017.

[17] S. A. Aghdam, "A novel UWB monopole antenna with tunable notched behavior using varactor diode," *IEEE Antennas and Wireless Propagation Letters*, vol. 13, pp. 1243–1246, 2014.

[18] P. Wang, G.-J. Wen, Y.-J. Huang, and Y.-H. Sun, "Compact CPW-fed planar monopole antenna with distinct triple bands for WiFi/WiMAX applications," *Electronics Letters*, vol. 48, no. 7, pp. 357–359, 2012.

[19] M. Sarkar, S. Dwari, and A. Daniel, "Printed monopole antenna for ultra-wideband application with tunable triple band-notched characteristics," *Wireless Personal Communications*, vol. 84, no. 4, pp. 2943–2954, 2015.

[20] P. Gao, L. Xiong, J. Dai, S. He, and Y. Zheng, "Compact printed wide-slot UWB antenna with 3.5/5.5-GHz dual band-notched characteristics," *IEEE Antennas and Wireless Propagation Letters*, vol. 12, pp. 983–986, 2013.

[21] T. Li, H. Zhai, G. Li, L. Li, and C. Liang, "Compact UWB band-notched antenna design using interdigital capacitance loading loop resonator," *IEEE Antennas and Wireless Propagation Letters*, vol. 11, pp. 724–727, 2012.

[22] W. T. Li, Y. Q. Hei, W. Feng, and X. W. Shi, "Planar antenna for 3G/Bluetooth/WiMAX and UWB applications with dual band-notched characteristics," *IEEE Antennas and Wireless Propagation Letters*, vol. 11, pp. 61–64, 2012.

[23] C. Wang, X. Wei, B. Ding et al., "A band-notched UWB slot antenna with high skirt selectivity and controllable bandwidth," in *2014 15th International Conference on Electronic Packaging Technology*, pp. 1237–1240, Chengdu, China, August 2014.

[24] Q. X. Chu, C. X. Mao, and H. Zhu, "A compact notched band UWB slot antenna with sharp selectivity and controllable bandwidth," *IEEE Transactions on Antennas and Propagation*, vol. 61, no. 8, pp. 3961–3966, 2013.

[25] Z. Tu, W.-A. Li, and Q.-X. Chu, "Single-layer differential CPW-fed notch-band tapered-slot UWB antenna," *IEEE Antennas and Wireless Propagation Letters*, vol. 13, pp. 1296–1299, 2014.

[26] A. D. Yaghjian and S. R. Best, "Impedance, bandwidth, and Q of antennas," *IEEE Transactions on Antennas and Propagation*, vol. 53, no. 4, pp. 1298–1324, 2005.

[27] J. Liang, C. C. Chiau, X. Chen, and C. G. Parini, "Printed circular disc monopole antenna for ultra-wideband applications," *Electronics Letters*, vol. 40, no. 20, pp. 1246-1247, 2004.

[28] A. B. Constantine, "Antenna theory: analysis and design," in *MICROSTRIP ANTENNAS, Third Edition*, John Wiley & Sons, 2005.

[29] O. Sydoruk, E. Tatartschuk, E. Shamonina, and L. Solymar, "Analytical formulation for the resonant frequency of split rings," *Journal of Applied Physics*, vol. 105, no. 1, article 014903, 2009.

[30] F. E. Terman, *Radio Engineers' Handbook*, McGraw-Hill Book, 1943.

[31] R. Garg, I. Bahl, and M. Bozzi, *Microstrip Lines and Slotlines*, Artech house, 2013.

[32] H. Zhai, L. Liu, Z. Ma, and C. Liang, "A printed monopole antenna for triple-band WLAN/WiMAX applications," *International Journal of Antennas and Propagation*, vol. 2015, Article ID 254268, 7 pages, 2015.

[33] K. A. Alshamaileh, M. J. Almalkawi, and V. K. Devabhaktuni, "Dual band-notched microstrip-fed Vivaldi antenna utilizing compact EBG structures," *International Journal of Antennas and Propagation*, vol. 2015, Article ID 439832, 7 pages, 2015.

[34] X. Chen, F. Xu, and X. Tan, "Design of a compact UWB antenna with triple notched bands using nonuniform width slots," *Journal of Sensors*, vol. 2017, Article ID 7673168, 9 pages, 2017.

[35] S. Das, D. Mitra, and S. R. B. Chaudhuri, "Design of UWB planar monopole antennas with etched spiral slot on the patch for multiple band-notched characteristics," *International Journal of Microwave Science and Technology*, vol. 2015, Article ID 303215, 9 pages, 2015.

[36] X. Li, L. Yan, W. Pan, and B. Luo, "A compact printed quadruple band-notched UWB antenna," *International Journal of Antennas and Propagation*, vol. 2013, Article ID 956898, 6 pages, 2013.

[37] D.-O. Kim, N.-I. Jo, H.-A. Jang, and C.-Y. Kim, "Design of the ultrawideband antenna with a quadruple-band rejection characteristics using a combination of the complementary split ring resonators," *Progress In Electromagnetics Research*, vol. 112, pp. 93–107, 2011.

[38] M. Rahman, D.-S. Ko, and J.-D. Park, "A compact multiple notched ultra-wide band antenna with an analysis of the CSRR-TO-CSRR coupling for portable UWB applications," *Sensors*, vol. 17, no. 10, p. 2174, 2017.